molecules still constitute a part of the bilayer assembly. Apparently, the dynamics of the entire system is sufficiently fast to produce these results. By proposing the involvement of lateral diffusion as a means of electron transport, we do not intend to exclude completely electron hopping in accounting for the full electroactivity of the system. We showed earlier for a similar system that translational diffusion is a dominant mechanism of the charge transport in bilayers.[7b] This finding may not be directly applicable to the present, more complicated case.

On the basis of this model, one might predict that the aggregation of $C_{18}Fc^+$ molecules around the immobilized GOd would leave some free space on the OTS surfaces. Consistent with this postulate, we found that the re-exposure of the $Au/Al_2O_3/OTS/C_{18}Fc^+/GOd$ electrode assembly to the original $C_{18}Fc^+$ loading solution resulted in a significant increase in the loading level of the ferrocene amphiphile. For example, in the case of the two electrodes mentioned above, the $C_{18}Fc^+$ loading increased 67% and 43% (compared to its initial value prior to the GOd immobilization) for the electrodes with GOd coverage of 3.3×10^{-13} and 1.3×10^{-13} mol/cm^2, respectively. This substantiates our aggregation model.

Conclusions

We have described here the structure and behavior of an organized multimolecular assembly designed to carry out enzymatically catalyzed electrooxidation of glucose. A key feature of this system is the immobilization of glucose oxidase in the head group region of an organized bilayer assembly. The electron transfer mediation of GOd is accomplished by the lateral diffusion of the octadecylferrocene amphiphile, one of the components of the bilayer. The overall electroenzymatic reaction is controlled by the lateral electron transport rate, or the kinetics of the mediation reaction. A simple analysis of the effect of GOd immobilization on the dynamics of the lateral diffusion suggests that the enzyme molecules aggregate around them a large number of the ferrocene surfactant molecules which remain electroactive but most likely do not participate in the lateral charge transport process. A number of important questions have emerged from this research. The issues concerning the kinetic aspects of this system as well as the questions addressing the nature of the $GOd/C_{18}Fc^+$ interactions and the structure of their aggregates are the subjects of our current investigations.

Acknowledgment. We gratefully acknowledge the National Science Foundation for supporting this research under Grant CHE-8807846. We acknowledge and thank NATO for the fellowship to C.B. during his sabbatical stay in Berkeley. We also thank Charles Goss for his assistance in the fabrication of the Au/Al_2O_3 electrodes.

Synthesis, Properties, and Molecular Structure of Highly Distorted Hexakis(trimethylsilyl)benzene[1]

Hideki Sakurai,* Keisuke Ebata, Chizuko Kabuto, and Akira Sekiguchi

Contribution from the Department of Chemistry and Organosilicon Research Laboratory, Faculty of Science, Tohoku University, Aoba-ku, Sendai 980, Japan. *Received April 10, 1989*

Abstract: Hexakis(trimethylsilyl)benzene (**2**), the most distorted benzene to a chair form, has been prepared as yellow crystals by methylation of hexakis(bromodimethylsilyl)benzene. The structure of **2** has been determined by X-ray crystallography. Crystals of **2** are orthorhombic, space group $P2_12_12_1$, a = 14.579 (3) Å, b = 18.927 (4) Å, c = 12.069 (9) Å, V = 3330.3 (10) Å^3, D_c = 1.02 g/cm^3, Z = 4. The benzene ring is remarkably deformed to a chair form with torsion angles of 9.8° (average) for C_{ar}–C_{ar}–C_{ar}–C_{ar}, and the six Si atoms are located up and down alternately from the benzene ring with torsion angles of 60.5° (average) for Si–C_{ar}–C_{ar}–Si. In solution, **2** exists as an equilibrium mixture of chair and boat forms. The quite unique chemical features of **2** are also demonstrated, for example, by photolysis with a light ($\lambda > 300$ nm) to afford hexakis(trimethylsilyl)bicyclo[2.2.0]hexa-2,5-diene (Dewar benzene), whereas thermolysis led to the formation of 1,1,3,4,6,6-hexakis(trimethylsilyl)-1,2,4,5-hexatetraene.

The molecular structures of overcrowded compounds are of interest in order to determine how the molecules relieve their inherent repulsive nonbonded interactions.[2] Hexa-*tert*-butylbenzene (**1**)[3] (Chart I) and hexakis(trimethylsilyl)benzene (**2**)[3,4] have not been synthesized yet, and hence, these sterically crowded molecules are one of the interesting synthetic targets. Hexakis(trimethylgermyl)benzene (**3**) has recently been prepared by Mislow and co-workers, and its unique molecular structure has been demonstrated.[3] The benzene ring of **3** distorts to a chair form in the ground state due to the nonbonded steric repulsion.[3,5] In contrast, the benzene ring of 1,3,5-tris(*N*,*N*-dialkylamino)-2,4,6-trinitrobenzene (**4**) highly distorts to a boat form by both steric and electronic reasons.[6]

(1) Chemistry of Organosilicon Compounds. 263.

(2) (a) Greenberg, A.; Liebman, J. F. *Strained Organic Molecules*; Academic Press: New York, 1978. (b) Tidwell, T. T. *Tetrahedron* **1978**, *34*, 1855.

(3) For the empirical force field calculations of hexa-*tert*-butylbenzene (**1**), hexakis(trimethylsilyl)benzene (**2**), and hexakis(trimethylgermyl)benzene (**3**) and for the X-ray crystal structure of **3** see: Weissensteiner, W.; Schuster, I. I.; Blount, J. F.; Mislow, K. *J. Am. Chem. Soc.* **1986**, *108*, 6664.

(4) The preparation of **2** was previously attempted. (a) Shiina, K.; Gilman, H. *J. Am. Chem. Soc.* **1966**, *88*, 5367. (b) Fearon, F. W. G.; Gilman, H. *Chem. Commun.* **1967**, 86. (c) Brennan, T.; Gilman, H. *J. Organomet. Chem.* **1968**, *11*, 625. (d) Ballard, D.; Brennan, T.; Fearon, F. W. G.; Shiina, K.; Haiduc, I.; Gilman, H. *Pure Appl. Chem.* **1969**, *19*, 449.

(5) Distorsions of benzenes into chair, twist, and boat forms have been studied. For chair form see: (a) Couldwell, M. H.; Penfold, B. R. *J. Cryst. Mol. Struct.* **1976**, *6*, 59. See also ref 3 and the references cited therein. For twist form see: (a) Mizuno, H.; Nishiguchi, K.; Toyoda, T.; Otsubo, T.; Misumi, S.; Morimoto, N. *Acta Crystallogr., Sec. B: Struct. Sci.* **1977**, *B33*, 329. (b) Pascal, R. A., Jr.; McMillan, W. D.; Van Engen, D.; Eason, R. G. *J. Am. Chem. Soc.* **1987**, *109*, 4660. For boat form see: (a) Cram, D. J.; Cram, J. M. *Acc. Chem. Res.* **1971**, *4*, 204. (b) Keehn, P. M.; Rosenfeld, S. M. *Cyclophanes*; Academic Press: New York, 1983. (c) Maas, G.; Fink, J.; Wingert, H.; Blatter, K.; Regitz, M. *Chem. Ber.* **1987**, *120*, 819.

(6) Chance, J. M.; Kahr, B.; Buda, A. B.; Siegel, J. S. *J. Am. Chem. Soc.* **1989**, *111*, 5940. We thank Professor Siegel for sending us a preprint and valuable comments.

0002-7863/90/1512-1799$02.50/0

Chart I

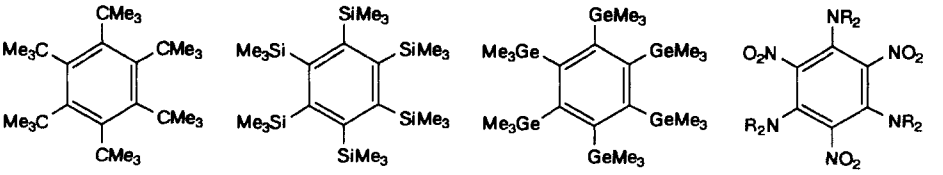

1 2 3 4

Scheme I

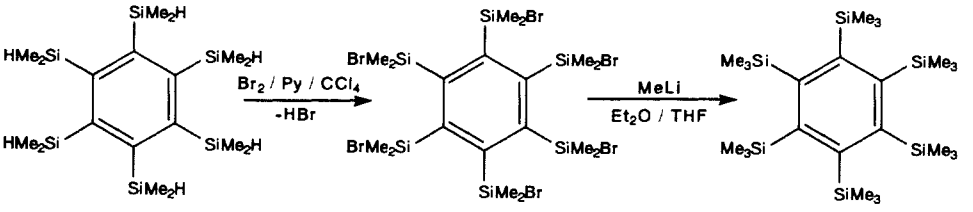

5 6 2

In connection with our studies on highly crowded silylethylenes,[7] it is quite interesting to investigate the physical and chemical properties of **2**. In this paper we report experimental details for the preparation and characterization of hitherto unknown hexakis(trimethylsilyl)benzene (**2**). The molecular structure determined by X-ray diffraction, in addition to its unusual chemical properties, will also be described.

Results and Discussion

Synthesis and Properties of Hexakis(trimethylsilyl)benzene (2). The preparation of **2** was previously attempted by treating hexabromobenzene with magnesium and chlorotrimethylsilane, but the reaction resulted in the formation of 1,1,3,4,6,6-hexakis(trimethylsilyl)-1,2,4,5-hexatetraene.[4c] Our strategy for the synthesis of **2** is outlined in Scheme I.[8]

Hexakis(dimethylsilyl)benzene (**5**),[4c] prepared by the method of Gilman from hexabromobenzene with magnesium and chlorodimethylsilane, was subjected to bromination in carbon tetrachloride at 0 °C in the presence of pyridine, giving hexakis(bromodimethylsilyl)benzene (**6**) as relatively labile yellow crystals. Without purification, **6** was treated with an excess of methyllithium in THF. The reaction mixture was concentrated and then chromatographed on silica gel with hexane to afford bright yellow crystals of **2** in 10% yield (from **5**). Compound **2** is fairly stable to air and water but readily decomposes by acids to give 1,2,4,5-tetrakis(trimethylsilyl)benzene.

Compound **2** shows quite unique chemical features. Irradiation of **2** ($\lambda > 300$ nm) in hexane resulted in the formation of hexakis(trimethylsilyl)bicyclo[2.2.0]hexa-2,5-diene (**7**) (Dewar benzene) (Scheme II). Dewar benzene **7** was isolated as deep red crystals. The photolysis of **2** is extremely clean, and Dewar benzene is formed quantitatively.

In the ^{13}C NMR spectrum of **7**, characteristic signals of the quarternary carbons and vinyl carbons appear at 75.2 and 173.8 ppm, respectively.[9] Dewar benzene **7** is a thermally labile molecule and is readily reverted to **2** by heating in solid state or in solution. The half-life is $t_{1/2}$ = 30.5 min at 86 °C (first-order rate constant, $k = 3.78 \times 10^{-4}$ s^{-1}) in toluene-d_8. Figure 1 shows

Scheme II

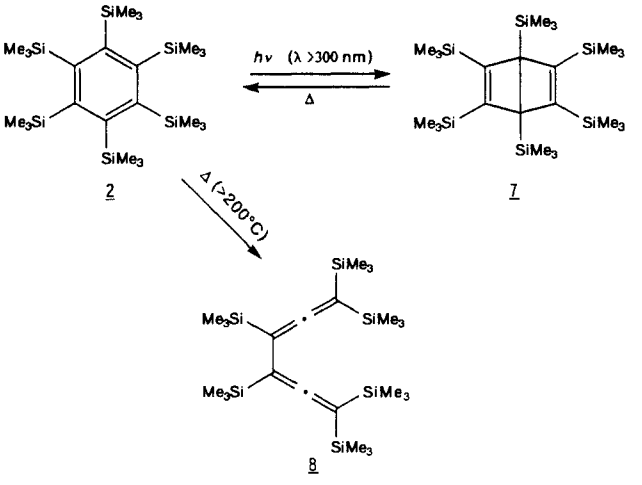

2 7 8

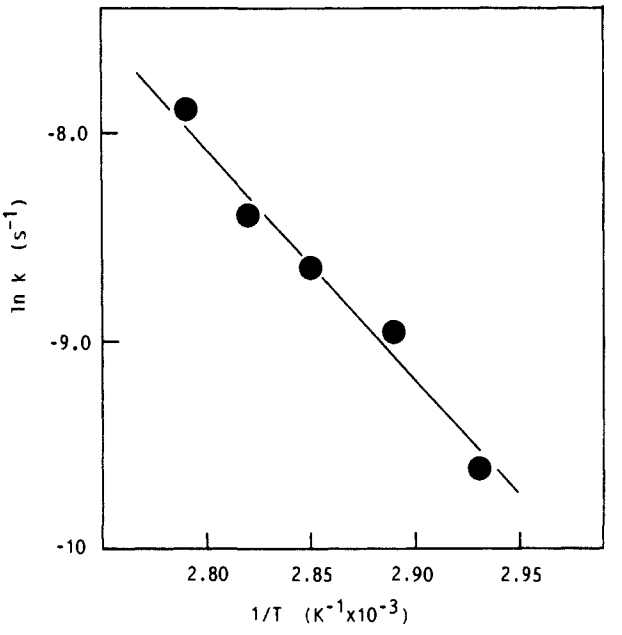

Figure 1. Eyring plot (ln k vs $1/T$) for the reaction of Dewar benzene **7** → hexakis(trimethylsilyl)benzene (**2**). The first-order rate constants $k \times 10^4$ s are 3.78 (86 °C), 2.24 (82 °C), 1.79 (78 °C), 1.32 (73 °C), and 0.68 (67 °C). The correlation coefficient is 0.990.

the Eyring plot, ln k vs $1/T$. Least-squares analysis gives the activation parameters: E_a = 21.2 kcal/mol, $\Delta G^{\ddagger}$ = 25.2 kcal/mol (25 °C), $\Delta H^{\ddagger}$ = 20.6 kcal/mol, $\Delta S^{\ddagger}$ = −15.3 eu.

(7) (a) Sakurai, H.; Nakadaira, Y.; Kira, M.; Tobita, H. *Tetrahedron Lett.* **1980**, *21*, 3077. (b) Sakurai, H.; Tobita, H.; Kira, M.; Nakadaira, Y. *Angew. Chem., Int. Ed. Engl.* **1980**, *19*, 620. (c) Sakurai, H.; Nakadaira, Y.; Tobita, H.; Ito, T.; Toriumi, K.; Ito, H. *J. Am. Chem. Soc.* **1982**, *104*, 300. (d) Sakurai, H.; Tobita, H.; Nakadaira, Y.; Kabuto, C. *J. Am. Chem. Soc.* **1982**, *104*, 4288. (e) Sakurai, H.; Ebata, K.; Nakadaira, Y.; Kabuto, C. *Chem. Lett.* **1987**, 301. (f) Sakurai, H.; Ebata, K.; Sakamoto, K.; Nakadaira, Y.; Kabuto, C. *Chem. Lett.* **1988**, 965. (g) Sekiguchi, A.; Nakanishi, T.; Kabuto, C.; Sakurai, H. *J. Am. Chem. Soc.* **1989**, *111*, 3748.

(8) We have also examined the reaction of hexabromobenzene with (trimethylsilyl)lithium in THF/HMPA, but none of **2** was obtained. The reaction of hexakis(dimethylsilyl)benzene (**5**) with diazomethane also failed.

(9) For the chemical shifts of the bridgehead quarternary carbons of the Dewar benzene derivatives see: (a) Wingert, H.; Maas, G.; Regitz, M. *Tetrahedron* **1986**, *42*, 5341. (b) Wingert, H.; Irngartinger, H.; Kallfa, D.; Regitz, M. *Chem. Ber.* **1987**, *120*, 825.

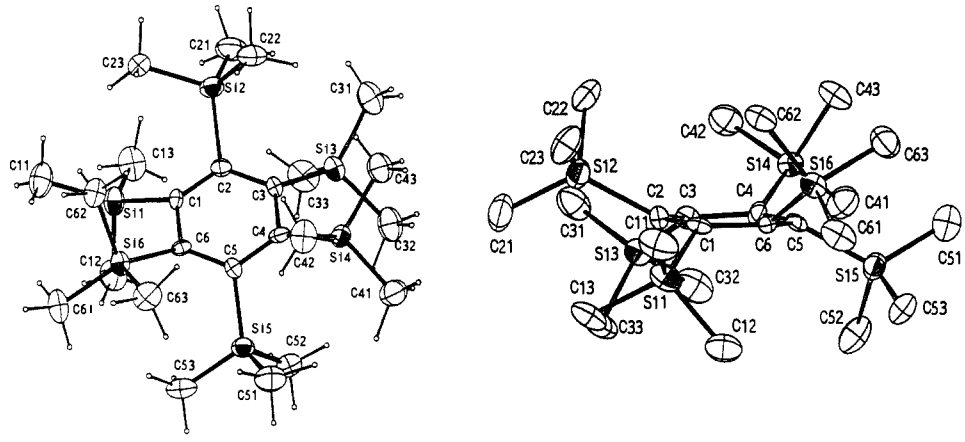

Figure 2. ORTEP drawing of **2** [top view (left), side view (right)].

Oth has reported the thermal isomerization of hexamethylbicyclo[2.2.0]hexa-2,5-diene (hexamethyl Dewar benzene) to hexamethylbenzene, with the following kinetic parameters: $k = 6.57 \times 10^{-5}$ s^{-1} (150 °C), $E_a = 37.2$ kcal/mol, $\Delta G^{\ddagger} = 33.2$ kcal/mol, $\Delta H^{\ddagger} = 36.4$ kcal/mol, $\Delta S^{\ddagger} = 7.5$ eu.[10] Rather facile isomerization of **7**, reflected in the low value of the activation enthalpy, may be ascribed to the destabilization of the central bond of **7** due to the σ(Si–C)–σ^*(C–C)–σ(C–Si) conjugation. The large negative activation entropy reflects an increase of the steric bulkiness arising from the central bond scission in the transition state. In contrast to the photochemical reaction, thermolysis of **2** in octane at 200 °C cleanly produced 1,1,3,4,6,6-hexakis(trimethylsilyl)-1,2,4,5-hexatetraene (**8**) via the rupture of the benzene ring. Surprisingly, desilylation product was not observed at all.

Molecular Structure of 2. The structure of **2** was determined by X-ray crystallography. Compound **2** crystallizes in two forms: orange and yellow crystals. Two crystals are isomorphous, consisting of similar structures. The orange ones belong to the space group *Pbca*, and Si methyl groups are disordered. The yellow ones belong to the space group $P2_12_12_1$, with ordered Si methyl groups, and thus, the data collection was carried out at low temperature (−40 °C).

The 4 molecules in the unit cell sit in general positions but have approximate D_3 symmetry. An ORTEP drawing of **2** is shown in Figure 2, final atomic parameters are listed in Table I, and bond lengths, bond angles, and torsion angles are given in Table II. The X-ray crystallographic analysis of **2** reveals several kinds of distortions for the relief of steric interactions. As shown in Figure 2, four of the aromatic carbons (C(1), C(3), C(4), C(6) are nearly coplanar, while C(2) and C(5) carbons are located above and below the C(1)–C(3)–C(4)–C(6) plane by +0.107 and −0.105 Å, respectively. Consequently, the benzene ring is significantly deformed into a chair form with an average torsion angle of 9.8° for C_{ar}–C_{ar}–C_{ar}–C_{ar}; the folding angles such as C(1)–C(2)–C(3)/C(3)–C(4)–C(6)–C(1) are 8.5° (average). The C_{ar}–Si bonds bend from the connecting plane of C_{ortho}–C_{ipso}–C_{ortho} to the extent of 22.2° (average). Positions of the Si atoms deviate up and down alternately about the benzene ring, the torsion angles, Si–C_{ar}–C_{ar}–Si, being as large as 60.5° (average). Bond lengths for C_{ar}–C_{ar} (average 1.413 Å) and Si–C_{ar} (average 1.922 Å) are slightly longer than the normal values (1.39 and 1.87 Å, respectively). The Si–C bonds (average 1.870 Å) are close to the normal, but the C_{ar}–Si–C angles are expanded to some extent (average 121.6°).

The molecular structure of **2** closely resembles that of hexakis(trimethylgermyl)benzene (**3**), but the magnitude of the distortion is greater than for **3** (6.8° for C_{ar}–C_{ar}–C_{ar}–C_{ar} torsion angle; 57.1° for Ge–C_{ar}–C_{ar}–Ge torsion angle).[3]

The calculated ground state of **2** has D_3 symmetry, and the overall present structural parameters by X-ray diffraction are roughly in accord with the calculated ones by the empirical force field method (EFF).[3] However, a closer look reveals some discrepancy. The bond lengths and torsion angles for Si–C_{ar}–C_{ar}–Si and C_{ar}–C_{ar}–C_{ar}–C_{ar} deviate markedly from the calculated ones. One of the reasons for this discrepancy is the inadequate Si parameters for calculating the highly distorted molecules. Despite the repeated attempts, the X-ray crystal structure determination of **7** failed at this moment.

Table I. Final Atomic Parameters for **2**[a,b]

atom	x	y	z
Si(1)	0.8887 (3)	0.3514 (2)	0.5287 (4)
Si(2)	0.9397 (3)	0.4755 (2)	0.7527 (4)
Si(3)	0.8964 (3)	0.6334 (2)	0.5926 (4)
Si(4)	1.1206 (3)	0.6406 (2)	0.4601 (3)
Si(5)	1.0693 (3)	0.5155 (2)	0.2422 (4)
Si(6)	1.1138 (3)	0.3583 (2)	0.4067 (4)
C(1)	0.9761 (8)	0.4294 (5)	0.5331 (10)
C(2)	0.9548 (8)	0.4875 (7)	0.5948 (11)
C(3)	0.9771 (9)	0.5575 (7)	0.5562 (11)
C(4)	1.0363 (9)	0.5639 (6)	0.4629 (10)
C(5)	1.0569 (7)	0.5036 (6)	0.3978 (10)
C(6)	1.0313 (8)	0.4358 (6)	0.4378 (9)
C(11)	0.923 (1)	0.259 (1)	0.571 (1)
C(12)	0.851 (1)	0.349 (1)	0.383 (1)
C(13)	0.781 (1)	0.374 (1)	0.605 (1)
C(21)	0.831 (1)	0.501 (1)	0.827 (2)
C(22)	1.038 (1)	0.528 (1)	0.815 (2)
C(23)	0.963 (1)	0.384 (1)	0.797 (2)
C(31)	0.902 (1)	0.679 (1)	0.730 (2)
C(32)	0.902 (1)	0.704 (1)	0.484 (2)
C(33)	0.780 (1)	0.595 (1)	0.577 (2)
C(41)	1.117 (1)	0.708 (1)	0.348 (2)
C(42)	1.120 (1)	0.690 (1)	0.596 (1)
C(43)	1.238 (1)	0.595 (1)	0.460 (1)
C(51)	1.175 (1)	0.551 (1)	0.182 (2)
C(52)	0.973 (1)	0.577 (1)	0.206 (2)
C(53)	1.042 (1)	0.437 (1)	0.163 (1)
C(61)	1.078 (1)	0.280 (1)	0.323 (1)
C(62)	1.150 (1)	0.327 (1)	0.545 (1)
C(63)	1.225 (1)	0.393 (1)	0.342 (1)

[a] Atomic numbers are given in Figure 2. Standard deviations are in parentheses. [b] Anisotropic thermal parameters and final atomic parameters for hydrogen are given in the supplementary material.

Physical Properties and Dynamics. We have examined the variable NMR and UV spectral experiments to see whether the structure found in the crystals persists in solution. Interestingly, NMR and UV spectra reveal that **2** exists as an equilibrium mixture consisting of the conformational isomers **2a** and **2b**. The ratios of **2a** to **2b** are 96/4 at 253 K, 92/8 at 273 K, 89/11 at 293 K, and 74/26 at 333 K in toluene-d_8.[11] This dynamic process was reversible, and the coalescence temperature (T_c) was 343 K (Figure 3). The aryl carbons of **2a** and **2b** are observed at 162.3 and 148.9 ppm, respectively.

(10) Oth, J. M. F. *Recl. Trav. Chim. Pays-Bas.* **1968**, *87*, 1185.

(11) The dynamic ^{1}H NMR spectra of **2** in toluene-d_8 were obtained on a Bruker AC-300 spectrometer in the temperature range 193–363 K. Hexakis(trimethylgermyl)benzene (**3**) did not show the dynamic behavior found in **2**.

Table II. Structural Parameters for 2

atoms	exptl (X-ray)	calcd (EFF)[3]	atoms	exptl (X-ray)	calcd (EFF)[3]	atoms	exptl (X-ray)	calcd (EFF)[3]
			Bond Lengths (Å)					
Si(1)–C(1)	1.951 (13)	1.885	Si(3)–C(32)	1.870 (18)		Si(6)–C(6)	1.935 (12)	
Si(1)–C(11)	1.893 (18)	1.859	Si(3)–C(33)	1.855 (18)		Si(6)–C(61)	1.868 (18)	
Si(1)–C(12)	1.843 (18)	1.906	Si(4)–C(4)	1.903 (12)		Si(6)–C(62)	1.855 (16)	
Si(1)–C(13)	1.872 (18)	1.890	Si(4)–C(41)	1.858 (18)		Si(6)–C(63)	1.909 (18)	
Si(2)–C(2)	1.933 (13)		Si(4)–C(42)	1.894 (18)		C(1)–C(2)	1.363 (18)	1.410
Si(2)–C(21)	1.879 (21)		Si(4)–C(43)	1.922 (18)		C(1)–C(6)	1.409 (16)	
Si(2)–C(22)	1.901 (18)		Si(5)–C(5)	1.900 (12)		C(2)–C(3)	1.442 (18)	1.413
Si(2)–C(23)	1.849 (18)		Si(5)–C(51)	1.833 (20)		C(3)–C(4)	1.424 (18)	
Si(3)–C(3)	1.908 (13)		Si(5)–C(52)	1.874 (20)		C(4)–C(5)	1.418 (18)	
Si(3)–C(31)	1.868 (18)		Si(5)–C(53)	1.817 (18)		C(5)–C(6)	1.420 (16)	
			Bond Angles (deg)					
C(1)–Si(1)–C(11)	121.4 (7)	121.8	C(4)–Si(4)–C(41)	121.2 (7)		Si(1)–C(1)–C(2)	118.5 (9)	118.3
C(1)–Si(1)–C(12)	103.6 (7)	104.2	C(4)–Si(4)–C(42)	111.4 (6)		Si(1)–C(1)–C(6)	114.6 (8)	117.4
C(1)–Si(1)–C(13)	111.3 (7)	114.5	C(4)–Si(4)–C(43)	103.4 (6)		C(2)–C(1)–C(6)	120.4 (11)	
C(11)–Si(1)–C(12)	108.6 (8)	109.4	C(41)–Si(4)–C(42)	107.0 (8)		Si(2)–C(2)–C(1)	118.0 (9)	
C(11)–Si(1)–C(13)	107.5 (8)	107.1	C(41)–Si(4)–C(43)	109.3 (7)		Si(2)–C(2)–C(3)	116.9 (9)	
C(12)–Si(1)–C(13)	102.8 (8)	96.7	C(42)–Si(4)–C(43)	103.1 (7)		C(1)–C(2)–C(3)	120.9 (11)	120.0
C(2)–Si(2)–C(21)	122.2 (7)		C(5)–Si(5)–C(51)	121.0 (7)		Si(3)–C(3)–C(2)	118.6 (9)	
C(2)–Si(2)–C(22)	104.0 (7)		C(5)–Si(5)–C(52)	103.3 (7)		Si(3)–C(3)–C(4)	119.5 (9)	
C(2)–Si(2)–C(23)	111.9 (7)		C(5)–Si(5)–C(53)	113.4 (7)		C(2)–C(3)–C(4)	118.0 (11)	
C(21)–Si(2)–C(22)	108.3 (8)		C(51)–Si(5)–C(52)	108.5 (8)		Si(4)–C(4)–C(3)	118.0 (9)	
C(21)–Si(2)–C(23)	105.1 (8)		C(51)–Si(5)–C(53)	106.2 (8)		Si(4)–C(4)–C(5)	117.9 (9)	
C(22)–Si(2)–C(23)	103.9 (8)		C(52)–Si(5)–C(53)	102.7 (8)		C(3)–C(4)–C(5)	119.9 (11)	
C(3)–Si(3)–C(31)	121.7 (7)		C(6)–Si(6)–C(61)	122.0 (6)		Si(5)–C(5)–C(4)	118.1 (9)	
C(3)–Si(3)–C(32)	110.5 (7)		C(6)–Si(6)–C(62)	104.3 (6)		Si(5)–C(5)–C(6)	118.0 (8)	
C(3)–Si(3)–C(33)	104.4 (7)		C(6)–Si(6)–C(63)	110.4 (6)		C(4)–C(5)–C(6)	118.9 (11)	
C(31)–Si(3)–C(32)	107.0 (8)		C(61)–Si(6)–C(62)	108.0 (7)		Si(6)–C(6)–C(1)	116.7 (8)	
C(31)–Si(3)–C(33)	107.9 (8)		C(61)–Si(6)–C(63)	106.8 (7)		Si(6)–C(6)–C(5)	117.1 (8)	
C(32)–Si(3)–C(33)	104.1 (8)		C(62)–Si(6)–C(63)	103.8 (7)		C(1)–C(6)–C(5)	120.4 (10)	
			Torsion Angles (deg)					
Si(1)–C(1)–C(2)–Si(2)	62.3	52.1	Si(4)–C(4)–C(5)–Si(5)	59.9		C(1)–C(2)–C(3)–C(4)	11.3	4.3
Si(1)–C(1)–C(6)–Si(6)	63.7		Si(5)–C(5)–C(6)–Si(6)	61.6		C(2)–C(3)–C(4)–C(5)	12.4	
Si(2)–C(2)–C(3)–Si(3)	57.1		C(6)–C(1)–C(2)–C(3)	8.7		C(3)–C(4)–C(5)–C(6)	11.0	
Si(3)–C(3)–C(4)–Si(4)	58.3		C(2)–C(1)–C(6)–C(5)	7.1		C(4)–C(5)–C(6)–C(1)	8.2	

atoms	exptl (X-ray)	atoms	exptl (X-ray)
Dihedral Angles (deg)			
C(1)–C(2)–C(3)/C(1)–C(3)–C(4)–C(6)	8.8	C(1)–C(6)–C(5)/C(1)–C(2)–C(4)–C(5)	6.7
C(4)–C(5)–C(6)/C(1)–C(3)–C(4)–C(6)	8.3	C(3)–C(4)–C(5)/C(2)–C(3)–C(5)–C(6)	10.3
C(2)–C(3)–C(4)/C(1)–C(2)–C(4)–C(5)	10.2	C(6)–C(1)–C(2)/C(2)–C(3)–C(5)–C(6)	6.8
Angles (deg)			
Si(1)–C(1)/C(6)–C(1)–C(2)	26.1	Si(4)–C(4)/C(3)–C(4)–C(5)	20.6
Si(2)–C(2)/C(1)–C(2)–C(3)	20.5	Si(5)–C(5)/C(4)–C(5)–C(6)	22.0
Si(3)–C(3)/C(2)–C(3)–C(4)	19.5	Si(6)–C(6)/C(5)–C(6)–C(1)	24.7

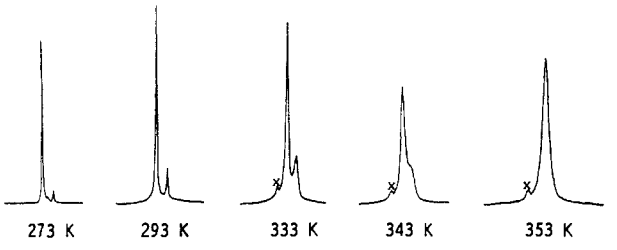

Figure 3. Variable-temperature ^{1}H NMR spectra of **2** 273, 293, 333, 343, and 353 K. The signal marked x is H_2O.

The abundant isomer in solution, **2a**, should have a chair form as determined in the crystals, since a solid-state ^{13}C NMR spectrum showed signals at 5.93 (SiMe) and 162.4 ppm (aromatic C) only. Compound **2b** may have either a boat structure **9** with D_2 symmetry or a planar structure **10** with S_6 symmetry (Chart II).

The EFF calculation also predicts the existence of two conformers: D_3 ground-state conformer of a chair form and the higher energy conformer with S_6 symmetry.[3] We prefer boat structure **9** because **2** readily gives Dewar benzene **7**.[12]

(12) Heat of formations for chair, boat, and planar hexakis(trimethylsilyl)benzenes were derived by PM3 calculations to be −177.7, −167.7, and −136.4 kcal/mol, respectively, with geometries obtained by MM2 calculations. Details of the calculation together with results of our own EFF calculations will be reported elsewhere.

Chart II

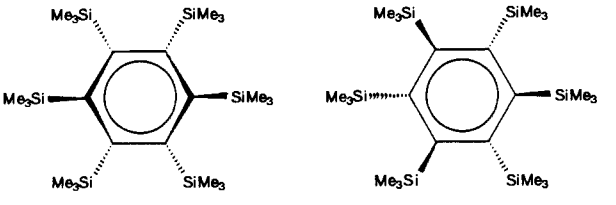

9 10

The fluxional rapid interconversion between the boat forms leads to the equivalence of the six trimethylsilyl groups in the NMR time scale. Thus, the dynamic process of **2** in solution reflects the conformational interconversion between the chair and boat forms. The free energy difference between these isomers is 4.73 kcal/mol.

The conformational equilibrium is also shown by the variable-temperature UV spectra of **2** (Figure 4). When the temperature is raised, the intensity of the absorption band at 318 nm decreases with concomitant increase of one at 277 nm. The latter band almost disappeared at −20 °C. These spectral changes are in good agreement with those of the dynamic NMR. The absorption band attibutable to **2b** could not be seen in the solid state (KBr tablet).

Experimental Section

General Methods. ^{1}H NMR spectra were recorded on a Bruker AC-300 FT spectrometer. ^{13}C and ^{29}Si NMR spectra were collected on a

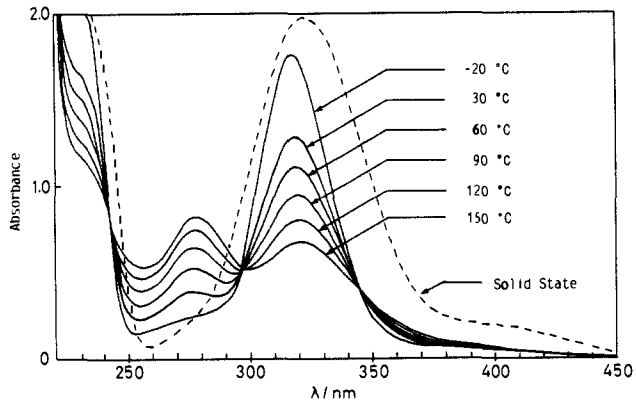

Figure 4. Variable-temperature electronic absorption spectra of **2** in decane (—) (-20, 30, 60, 90, 120, 150 °C) and in KBr (···) (25 °C).

Bruker AC-300 at 75.5 and 59.6 MHz, respectively. Chemical shifts are based on the residual solvent resonances. Mass spectra and high-resolution mass spectra were obtained on a Shimadzu QP-1000 and JEOL JMS D-300 mass spectrometers. Electronic spectra were recorded on a Shimadzu UV-2100 spectrometer. Melting points are uncorrected. All solvents were dried and distilled from sodium benzophenone ketyl prior to use.

Preparation of Hexakis(dimethylsilyl)benzene (5). Hexakis(dimethylsilyl)benzene (**5**) was prepared in 43% yield by the method of Gilman using hexabromobenzene, chlorodimethylsilane, and magnesium in THF:[4c] mp 201–202 °C; ^{1}H NMR (C_6D_6, δ) 0.54 (36 H, d, J = 3.7 Hz, $SiMe_2$), 4.99 (6 H, sept, J = 3.7 Hz, SiH); ^{13}C NMR (C_6D_6, δ) 1.02, 154.6; ^{29}Si NMR (C_6D_6, δ) −18.8 ppm.

Preparation of Hexakis(bromodimethylsilyl)benzene (6). Bromine (13.5 g, 84.3 mmol) in CCl_4 (10 mL) was added to a mixture of hexakis(dimethylsilyl)benzene (**5**; 6.0 g, 14.1 mmol) and pyridine (60 mL) in CCl_4 (20 mL) with stirring under argon at 0 °C. The color of the bromine immediately disappeared, and the solution became yellow. The reaction mixture was stirred for the additional 5 h at 0 °C, and then the resulting pyridinium bromide was filtered off under argon. Evaporation of the solvent afforded hexakis(bromodimethylsilyl)benzene (**6**) as a yellow solid that could be recrystallized from hexane/benzene: mp 221–223 °C dec; ^{1}H NMR (C_6D_6, δ) 1.00 (s, $SiMe_2Br$); ^{13}C NMR (C_6D_6, δ) 9.63 (SiMe), 160.6 (aromatic C); ^{29}Si NMR (C_6D_6, δ) 14.2 ppm. Anal. Calcd for $C_{18}H_{36}Si_6Br_6$: C, 24.01; H, 4.03. Found: C, 23.94; H, 4.22.

Preparation of Hexakis(trimethylsilyl)benzene (2). To the above crude hexakis(bromodimethylsilyl)benzene (**6**) was added 90 mL of dry THF, and then an ether solution of methyllithium (100 mL, 0.108 mol) was added dropwise under argon. The solution became dark red. After being stirred overnight, the reaction mixture was poured into hexane and hydrolyzed with aqueous ammonium chloride followed by extraction with hexane. The organic layer was dried over anhydrous sodium sulfate and concentrated. The deep red oily residue was subjected to chromatography on silica gel with hexane to give a yellow fraction. Evaporation of the solvent afforded yellow crystals of hexakis(trimethylsilyl)benzene (**2**; 734 mg, 10.2%) that were recrystallized from ethanol: mp 216 °C; ^{1}H NMR (C_6D_6, δ) 0.34 (s, $SiMe_3$, **2b**), 0.39 (s, $SiMe_3$, **2a**); ^{13}C NMR (C_6D_6, δ) 5.09 ($SiMe_3$, **2a** and **2b**), 148.9 (aromatic C, **2b**), 162.3 (aromatic C, **2a**); ^{29}Si NMR (C_6D_6, δ) −6.41 (**2b**), −6.28 (**2a**); UV (hexane, 20 °C, λ_{max}/nm (ϵ)) 216 (30 000), 233 (sh, 12 000), 277 (2700), 318 (11 000); MS, m/z (%) 510 (M^+, 54), 437 (29), 155 (67), 73 (100); high-resolution MS for $C_{24}H_{54}Si_6$ calcd 510.2841, found 510.2840.

Photolysis of 2. A solution of **2** (400 mg, 0.784 mmol) and hexane (30 mL) was placed in a Pyrex tube and irradiated with a 500-W high-pressure mercury lamp for 1 h at room temperature through the cutoff filter (λ > 300 nm). The solution turned from yellow to dark red. NMR analysis showed the complete absence of **2**. Evaporation of the solvent gave the crude hexakis(trimethylsilyl)bicyclo[2.2.0]hexa-2,5-diene (**7**) in quantitative yield as deep red crystals that were recrystallized from ethanol: ^{1}H NMR (C_6D_6, δ) 0.28 (s, 18 H, $SiMe_3$), 0.29 (s, 36 H, $SiMe_3$); ^{13}C NMR (C_6D_6, δ) 2.33 ($SiMe_3$ × 4), 3.33 ($SiMe_3$ × 2), 75.2 (quarternary C), 173.8 (olefinic C); ^{29}Si NMR (C_6D_6, δ) −14.0 ($SiMe_3$ × 2), −7.46 ($SiMe_3$); UV (hexane, λ_{max}/nm (ϵ)) 471 (320); MS, m/z 510 (M^+, 15), 437 (7), 115 (19), 73 (100); high-resolution MS for $C_{24}H_{54}Si_6$ calcd 510.2841, found 510.2853.

Thermolysis of 2. A solution of **2** (34 mg, 0.067 mmol) and octane (2 mL) was heated in a sealed tube at 200 °C for 14 h. The solution turned colorless after thermolysis. NMR analysis of the reaction mixture showed the complete absence of **2**. Evaporation of the solvent gave 1,1,3,4,6,6-hexakis(trimethylsilyl)-1,2,4,5-hexatetraene (**8**) (34 mg, 100%) as colorless crystals. The structure of the product was identified by comparison of its spectral properties with the reported ones:[3,4c] mp 109–110 °C; ^{1}H NMR ($CDCl_3$, δ) 0.08 (s, 18 H, $SiMe_3$), 0.12 (s, 36 H, $SiMe_3$); ^{13}C NMR ($CDCl_3$, δ) 0.50, 0.54, 74.6, 79.5, 206.4.

X-ray Crystallography of 2. Diffraction data were collected on a Rigaku Denki AFC-5PR diffractometer with a rotating anode (45 kV, 200 mA) with graphite-monochromatized Mo Kα radiation (λ = 0.71069 Å). Crystals for X-ray analysis were obtained from ethanol/hexane solution. The data collection was carried out at low temperature (−40 °C) on a crystal of dimensions 0.15 × 0.20 × 0.25 mm. A total of 2601 reflections with 2θ = 50° were collected. Crystal data: MF = $C_{24}H_{54}Si_6$; MW = 511.19; orthorhombic; a = 14.579 (3), b = 18.927 (4), c = 12.069 (9) Å; V = 3330.3 (10) Å^3; space group = $P2_12_12_1$; Z = 4; D_c = 1.02 g/cm^3. The structure was refined anisotropically for Si and aromatic C atoms and isotropically for methyl C atoms. H atoms were not refined but included in F_c calculations. The final R factor was 0.078 (R_w = 0.078) for 1561 reflections with $F_0 > 2.5\sigma(F_0)$. The structure was solved by direct methods with the applied library program UNICS III[13] system and RANTAN81[14] direct-methods program. Tables of details of X-ray experiments, fractional atomic coordinates for silicon and aromatic carbon atoms, anisotropic temperature factors for nonhydrogen atoms, fractional atomic coordinates for hydrogen atoms, bond lengths, and bond angles and a list of observed and calculated structure factors are in the supplementary material.

Acknowledgment. We thank the Ministry of Education, Science and Culture (Grant-in-Aid for Special Project Research No. 62115003) for support of this work.

Supplementary Material Available: ORTEP drawing of hexakis(trimethylsilyl)benzene (Figure 2), and tables of details of X-ray experiments (Table 1), fractional atomic coordinates for silicon and aromatic carbon atoms (Table 2), anisotropic temperature factors for silicon and aromatic carbon atoms (Table 3), fractional atomic coordinates for methyl carbon and hydrogen atoms (Table 4), bond lengths (Table 5), and bond angles (Table 6) (7 pages); list of observed and calculated structure factors (Table 7) (9 pages). Ordering information is given on any current masthead page.

(13) Sakurai, T.; Kobayashi, K. *Rep. Inst. Phys. Chem. Res. (Jpn.)* **1979**, *55*, 69.

(14) (a) Jia-Xing, Y. *Acta Crystallogr., Sect. A: Cryst. Phys., Diffr., Theor. Gen. Crystallogr.* **1981**, *37*, 642. (b) *Ibid.* **1983**, *39*, 35.